resistance [2]. Aromatase inhibitors have recently replaced antiestrogens as a more appropriate hormonal therapy for advanced breast cancer and also in an adjuvant setting [3]. Although estrogen ablation is another effective strategy for ER-positive breast cancer, the acquisition of estrogen-deprivation resistance is one of the crucial steps in the progression to hormonal therapy resistance and more aggressive tumors in ERα-expressing breast cancer. The mechanisms for the estrogen-deprivation resistance of ERα-expressing breast cancer cells have also been explored by several laboratories [4–6] using whole cells cultured for a long-term period in estrogen-deprivation medium. These reports suggested that resistant cells acquired estrogen hypersensitivity by crosstalk with the MAP-kinase or PI3K-Akt pathway and the involvement of membrane-associated ER [7]. However, the precise mechanisms are not fully understood, and several questions remain unanswered in terms of whether any other mechanisms are associated with this resistance. To address these issues, we here established several MCF-7 cell sub-lines by isolating single colonies under long-term estrogen-deprivation conditions. MCF-7 cells stably transfected with the ERE-GFP reporter gene were used as parental cells for this cell cloning. These cells expressed GFP on ER activation, and ER activity was assessed in living cells by fluorescence [8,9]. Using this system, we eventually established the two types of clones as long-term estrogen depletion resistant (EDR) cell lines and characterized them. Our study indicated that more than two clearly distinct mechanisms exist in estrogen-deprivation resistance.

2. Materials and methods

2.1. Reagents

Estradiol (E2) and 4-hydroxytamoxifen were purchased from Sigma–Aldrich (St. Louis, MO, USA). Fulvestrant (Ful) and toremifene (TOR) were kindly provided by AstraZeneca Pharmaceuticals (London, UK) and Nippon Kayaku Co. Ltd. (Tokyo, Japan), respectively. The sources of antibodies for Western blotting were as follows: total ERα (H-184) from Santa Cruz Biotechnology Inc. (Santa Cruz, CA, USA), HER2 from DakoCytomation (Glostrup, Denmark), EGFR, phospho-ERα (Ser167), phospho-ERα (Ser118), total and phospho-p44/42 MAPK (Erk1/2), total and phospho-Akt (Thr308), total and phospho-JNK, β-tubulin, and the PI3K inhibitor, LY294002 from Cell Signaling Technology Inc. (Danvers, MA, USA). Secondary antibodies conjugated with alkaline phosphatase were purchased from Bio-Rad Laboratories Inc. (Hercules, CA, USA). The JNK inhibitor, SP600125, IGF-1R inhibitor, AG1024, and EGFR inhibitor, AG1478, were purchased from Cayman Chemical Company (Ann Arbor, MI, USA) or EMD Biosciences, Inc. (La Jolla, CA, USA).

2.2. Cells and cell culture

MCF-7-E10 cells were established from human breast cancer MCF-7 cells, into which the ERE-GFP reporter gene had been stably introduced. These cells expressed GFP in the presence of estrogen under fluorescence. MCF-7-E10 cells were routinely cultured in RPMI1640 medium (Sigma–Aldrich) containing 10% fetal calf serum (FCS; Tissue Culture Biologicals, Turale, CA, USA) and 1% penicillin/streptomycin (Sigma–Aldrich).

MCF-7-E10 cells were cultured in estrogen-deprived medium for 3 months. Among the surviving cells, ERE-GFP-expressing colonies and ERE-GFP-negative colonies were picked up separately and established as long-term estrogen-deprivation-resistant (EDR) cell lines. EDR cells were maintained in phenol red-free RPMI1640 medium (GIBCO BRL, Grand Island, NY, USA) supplemented with 10% dextran-coated charcoal-treated FCS (DCC-FCS) and 1% penicillin/streptomycin. All cells were incubated at 37 °C in a humidified atmosphere of 5% CO_2 in air. The characteristics of these cells did not change with the number of passages and cells that had gone through as low a number of passages as possible were used in the experiments of this study.

2.3. ERE-GFP assay

We assessed ERE activation by estimating GFP expression levels as reported previously [8–10]. Briefly, the number of cells expressing GFP was counted under fluorescence microscopy after the cells had been harvested by treatment with trypsin. Cells expressing strong levels of GFP were counted. ERE activity were expressed as the percentage of cells expressing GFP.

2.4. Cell growth assay

MCF-7-E10 cells (which had previously been stripped of steroids for 3 days by DCC-FCS-containing medium) and EDR cells were seeded at a density of 5×10^3 cells per well in a 24-well culture plate treated with the indicated concentrations of E2 for 4 days. Cells were counted using a CDA-500 Sysmex automated cell counter (Sysmex Corp., Kobe, Japan). Data are indicated as values relative to the cell numbers of the vehicle-treated control.

2.5. Real-time PCR

Total RNA was extracted from whole cells using Isogen (Nippon Gene Co., Ltd., Toyama, Japan) according to the manufacturer's instructions. Extracted RNA (1 μg) was converted to first-strand cDNA primed with a random hexamer in a 10 μl reaction volume using an RNA PCR kit (Takara Bio Inc., Otsu, Japan) and a 2 μl aliquot was used as a template for real-time PCR. All RNA quantification was carried out according to the standard protocol on an Applied Biosystems Step One real-time PCR system (Applied Biosystems Inc., Foster City, CA, USA). Target gene expression was normalized to *glyceraldehyde-3-phosphate dehydrogenase (GAPDH)*. All PCRs were performed at least twice and the results shown were from samples analyzed in triplicate in one experiment. These results confirmed the reproducibility of the data obtained. The sequences of the primer sets were as follows: *EGR3*-forward, 5′-GAG CAG TTT GCT AAA CCA AC-3′; reverse, 5′-AGA CCG ATG TCC ATT ACA TT-3′; *pS2*-forward, 5′-TCC CCT GGT GCT TCT ATC CTA A-3′; reverse, 5′-ACT AAT CAC CGT GCT GGG GA-3′; *PgR*-forward, 5′-AGC TCA CAG CGT TTC TAT CA-3′; reverse, 5′-CGG GAC TGG ATA AAT GTA TTC-3′; *Bcl-2*-forward, 5′-GTG GAT GAC TGA GTA CCT GAA C-3′; reverse, 5′-GCC AGG AGA AAT CAA ACA-3′; *CyclinD1*-forward, 5′-GGA GCC CGT GAA AAA GAG-3′; reverse, 5′-CAG GTT CCA CTT GAG CTT GT-3′; *GAPDH*-forward, 5′–ACA TCG CTC AGA CAC CAT GG-3′; reverse, 5′–GTA GTT GAG GTC AAT GAA GGG-3′.

2.6. Western blot analysis

Cell lysates were prepared using Lysis-M Reagent (Roche Diagnostics GmbH, Mannheim, Germany) supplemented with phosphatase inhibitor cocktails, Phos STOP (Roche Diagnostics), according to the manufacturer's instructions. Total proteins were run on SDS-PAGE using 10% acrylamide gels (SuperSep™ ace; Wako Pure Chemical Industries, Ltd., Osaka, Japan) and proteins were transferred to PVDF, Amersham Hybond™-P (GE Healthcare UK, Ltd., UK). The expression of proteins was determined by Western blotting with specific antibodies listed in *Reagents*, and expression signals using Immun-star AP substrate (Bio-Rad) were obtained by enhanced chemiluminescence. Densitometry was performed on three blots (two blots only in Fig. 4A) and these results

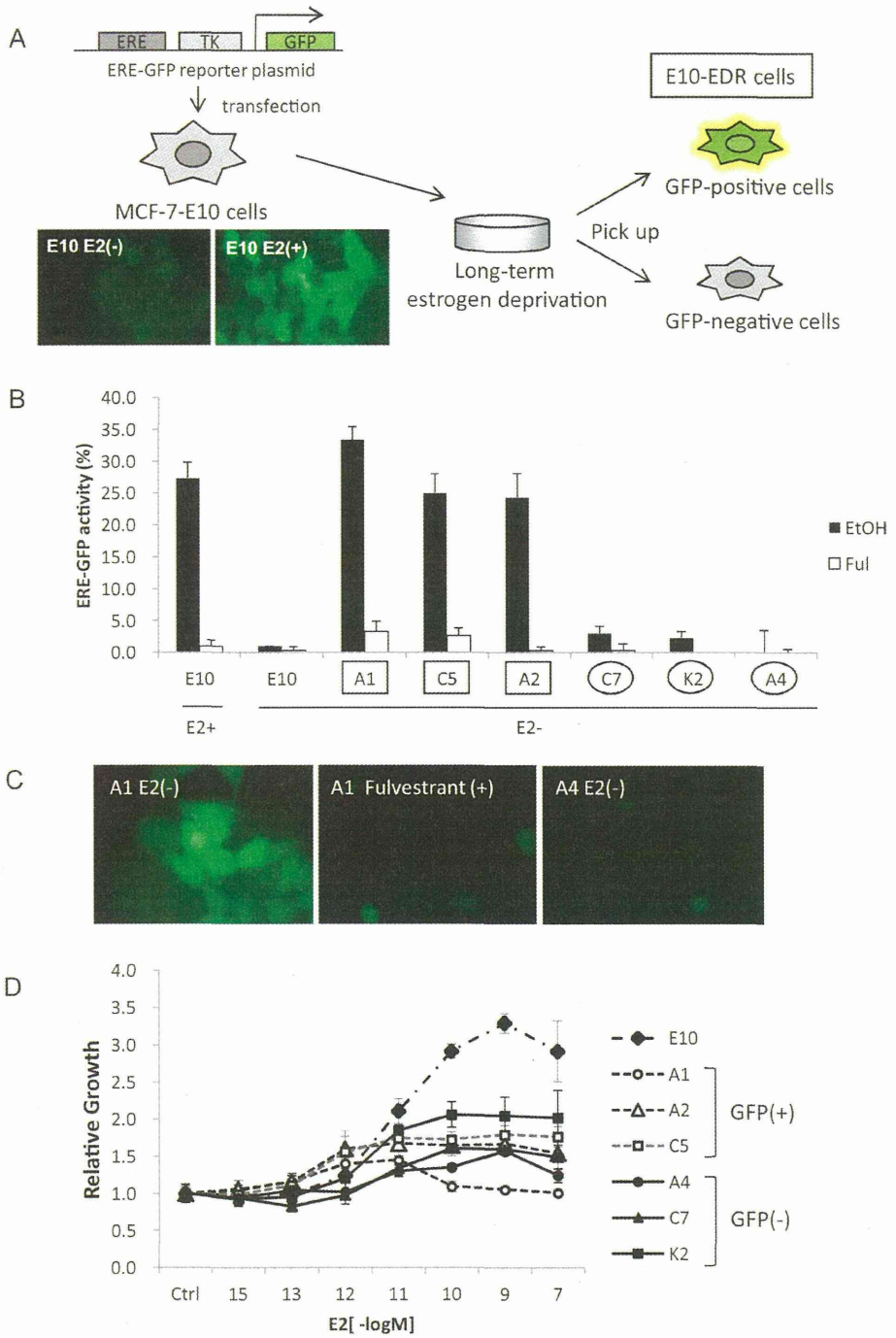

Fig. 1. Establishment of E10-EDR (estrogen-deprivation-resistant) cells. (A) MCF-7-E10 cells were cultured in RPMI1640 with 10% DCC-FCS for at least 3 months. Among the surviving cells, GFP-positive and GFP-negative colonies were isolated and established as long-term estrogen-deprivation-resistant (EDR) cell lines. (B) E10 and the isolated clones were treated with or without a pure antiestrogen (1 μM fulvestrant) in estrogen-deprived medium (E2−) and screened by counting the number of GFP-expressing cells. For comparison, E10 was performed with the same treatment in estrogen condition medium (E2+). As representative clones, three clones (A1, A2, C5) with high GFP expression and another three clones (A4, C7, K2) that did not show GFP expression were used for the following experiments. All data shown are means ± SD of these independent experiments. (C) Pictures of EDR cells under fluorescence microscopy. Examples of GFP-positive cells, A1 and treated with fulvestrant (1 μM) and GFP-negative cells A4 in the absence of estrogen. (D) EDR cells exhibited estrogen-independent growth. After 3 days of culture in RPMI1640 with 10% DCC-FCS, MCF-E10 and EDR cells were plated at 5×10^3 cells/well into 24-well plates and cultured in estrogen-deprived medium including a series of estrogen concentrations for 4 days. The number of cells was counted using a Coulter Counter. Data are indicated as values relative to the cell numbers with vehicle because the condition in which each cell can exhibit stationary proliferation is better as the control. All data are shown as means ± SD of three independent experiments.

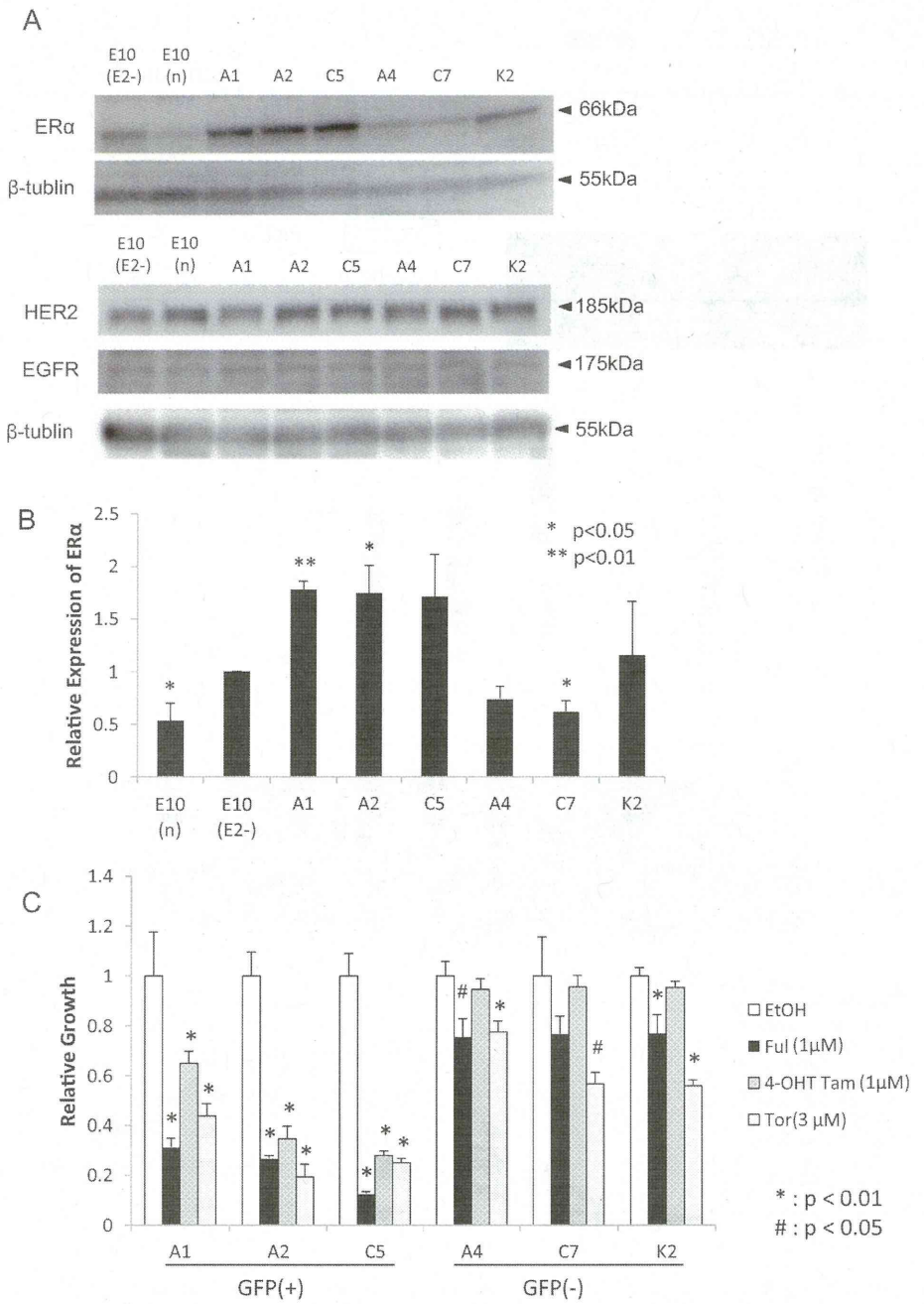

Fig. 2. Characterization of EDR cells. (A) Western blot analysis using whole-cell lysates from MCF-7-E10 and EDR cells was performed using antibodies against ERα, HER2, EGFR, and β-tubulin as described in Section 2. (B) Densitometry results on ERα blots. Densitometry was performed on three blots and the results were indicated as values relative to the intensity with E10 (E2−). Statistical analysis of the indicated averages was performed using the Student's *t*-test, $p < 0.01$ and $p < 0.05$. (C) Effect of antiestrogens on EDR cells. EDR cells (plated 1×10^4 cells/well into 24-well plate) were cultured in RPMI1640 with 10% DCC-FCS. The cells were incubated with the antiestrogen drugs, 1 μM fulvestrant (Ful), 1 μM 4-hydroxytamoxifen (4-OHT), and 3 μM toremifene (Tor) with ethanol (EtOH) as a control. The concentrations of antiestrogens were based on the concentration in the blood or tissue using a clinical dose. The number of cells was estimated after 4 days as described in Section 2. Data are indicated as values relative to the cell numbers with vehicle. All data are shown as means ± SD of three independent experiments.

are shown in figures, which indicated values as relative to the intensity obtained with E10 (E2−) or the controls as one.

2.7. AP-1 luciferase assay

AP-1 activity in MCF-7-E10 cells and EDR-E10 cells was measured using plasmids containing the AP-1 responsive element (TAAAAAAGCATGAGTCAGACACCTGAGCT) upstream of the collagenase gene in the pGL-2-promoter vector (Promega, Madison, WI, USA) and Dual-Luciferase Reporter System (Promega, Madison, WI, USA). MCF-7-E10 cells and EDR cells were seeded at a density of 5×10^4 cells per 6-cm dish in estrogen-deprived medium and cultured for 24 h. The AP-1-Luci plasmid (0.5 μg) and pRL-Luci plasmid (0.05 μg) were mixed with 5 μl of TransIT LT-1 reagent (Takara Bio

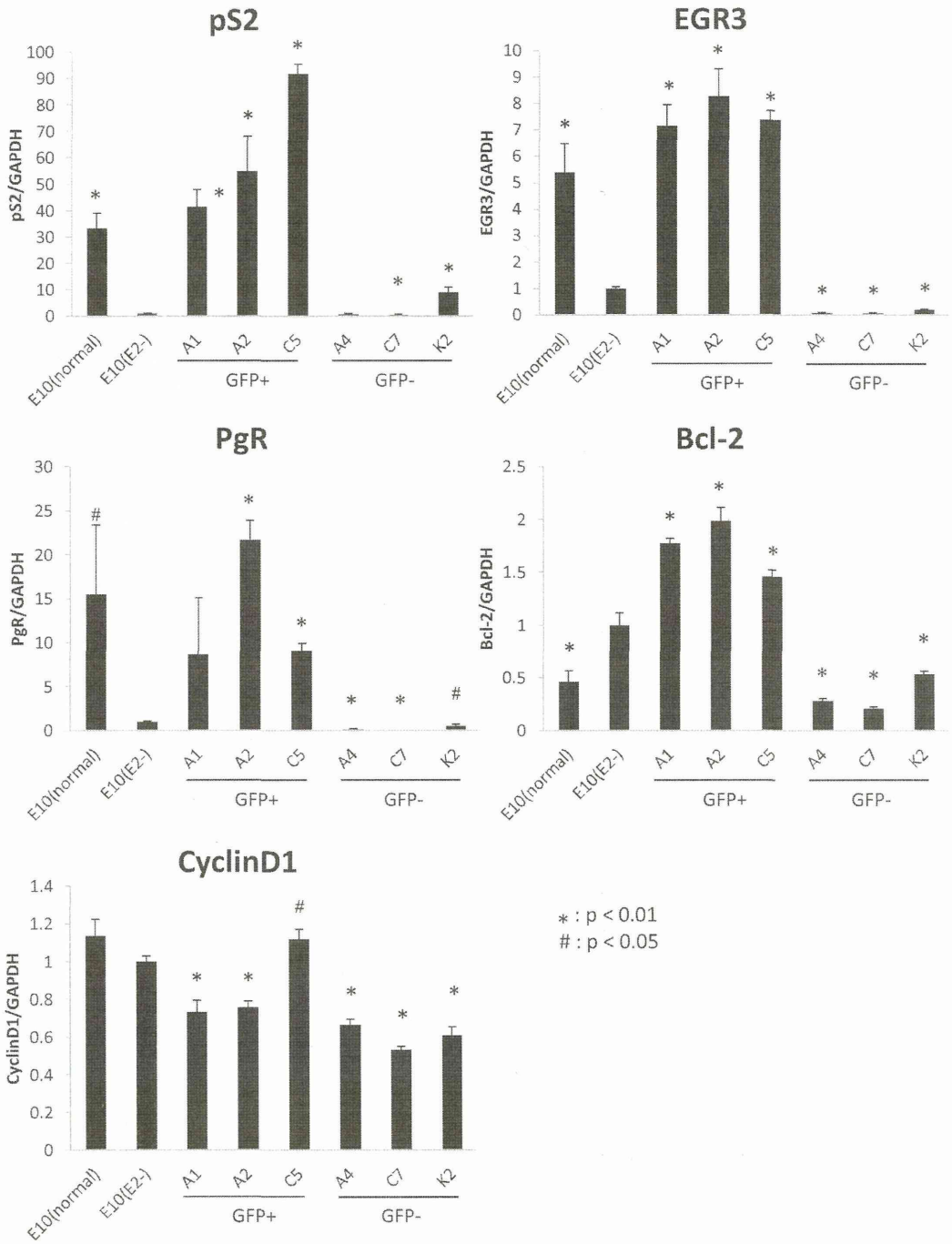

Fig. 3. The expression of ER-target genes. *pS2*, *EGR3*, *cyclinD1*, *progesterone receptor (PgR)*, and *Bcl-2* were measured by real-time PCR normalized to glyceraldehyde-3-phosphate dehydrogenase (GAPDH) in MCF-7-E10 and EDR cells. Total RNA extracted from MCF-7-E10 was cultured in normal RPMI1640 with 10% FCS (normal) or RPMI1640 with 10% DCC-FCS (E2−), and EDR cells was cultured in RPMI1640 with 10% DCC-FCS (E2−). Statistical analysis of the indicated averages was performed using the Student's *t*-test where $p < 0.05$ (#) or $p < 0.01$ (*) indicated a significant difference from E10 (E2−).

Inc.) in 300 μl of serum-free medium and subjected to transfection for 24 h. Luciferase activity was measured according to the manufacturer's instructions using the Dual-Luciferase Reporter Assay System (Promega).

2.8. GAL-4 reporter assay

The transcriptional activity of the A/B and E domains in ER was analyzed by luciferase assays using pCMX-GAL4-N-ER.A/B and pCMX-GAL4-N-ER.E expression plasmids, which contained a sequence encoding either the ER.A/B or ER.E region of ERα fused to the GAL4 DNA binding domain [11]. MCF-7-E10 cells and EDR cells were seeded at a density of 5×10^4 cells per 6-cm dish in estrogen-deprived medium and cultured for 24 h. After co-transfection with 0.05 μg of pCMX-GAL4-N-ER.A/B, 0.5 μg of tk-GALpx3-Luc, or 0.05 μg of the pRL-TK-Luc control plasmid with 5 μl of TransIT LT-1 reagent in DCC-FCS medium for 1 h, cells were treated with LY294002 (5 μM) and cultured for 24 h. Luciferase

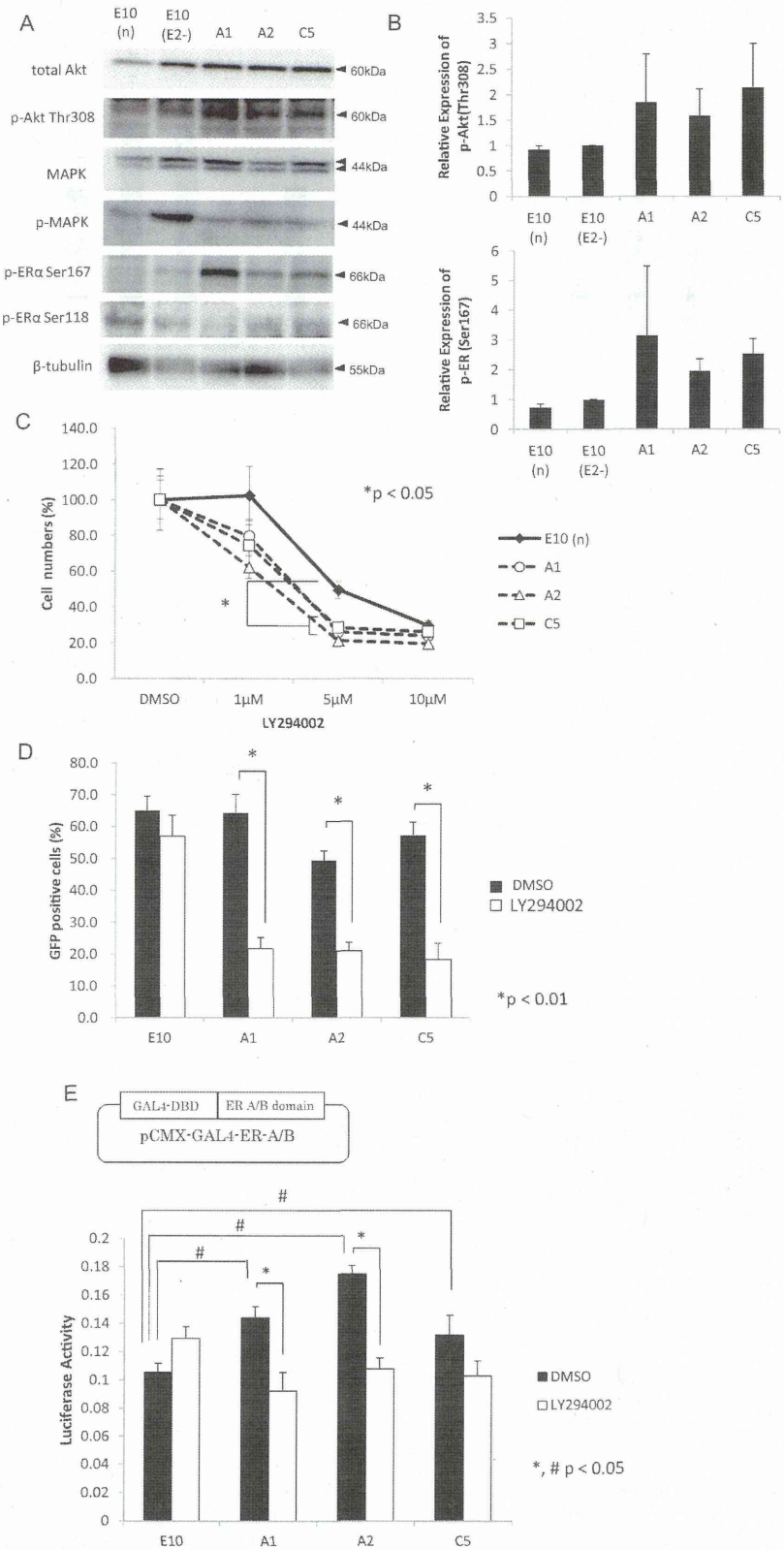

Fig. 4. The mechanisms of constitutive ER activation in GFP-positive EDR cells. (A) Western blot analysis using whole-cell lysates from MCF-7-E10 cells, which were cultured with RPMI1640 with 10% FCS (normal; *n*) or RPMI1640 with 10% DCC-FCS (E2−), as well as EDR cells, was performed using antibodies against total Erk1/2, p-Erk1/2, total Akt, p-Akt (Thr308), p-ERα (Ser167), p-ERα (Ser118), and β-tubulin as described in Section 2. (B) Densitometry results on p-Akt (Thr308) and p-ERα (Ser167) blots. Densitometry was performed on blots and the results were indicated as average values relative to the intensity with E10 (E2−). (C) The growth of GFP-positive cells was inhibited by the PI3K inhibitor. MCF-7-E10 cells were plated at 1.0×10^4 cells/well into a 24-well plate and were cultured in RPMI1640 with 10% FCS (normal). EDR cells (A1, A2, C5) were also plated at 1.0×10^4 cells/well into a 24-well plate and were cultured in RPMI1640 with 10% DCC-FCS. We set each medium so that E10 and EDR cells could proliferate

activity was measured twice and normalized with pRL-TK-Luc activity.

2.9. Mass spectrometry-based phosphoproteome analysis and KeyMolnet analysis

MCF-7-E10 cells and EDR cells (A1) were cultured in RPMI1640 with 10% FCS or phenol red-free RPMI1640 with 10% DCC-FCS, respectively, and cell lysates were harvested. Sample preparation for mass spectrometric analyses (i.e., cell lysate, protein extraction, protein digestion, phosphopeptide enrichment) was performed as described elsewhere [12]. Purified samples were then analyzed using an LTQ-Orbitrap mass spectrometer (Thermo Fisher Scientific, Waltham, MA, USA) [13]. Peptides and proteins were identified by means of an automated database search using Mascot version 2.2 (Matrix Science, London, UK) against UniProt/SwissProt release 56.0 with a precursor mass tolerance of 3 ppm, fragment ion mass tolerance of 0.8 Da, and strict trypsin specificity allowing for up to two missed cleavages. Cysteine carbamidomethylation was set as a fixed modification, and methionine oxidation and the phosphorylation of serine, threonine, and tyrosine were allowed as variable modifications. Peptides were considered to be identical if the Mascot score was over the 95% confidence limit based on the "identity" score of each peptide, and at least three successive y or b ions with two and more y, b, and/or precursor origin neutral loss ions were observed. Phosphorylated sites were unambiguously determined when y or b ions, between which the phosphorylated residue was located, were observed in the peak lists of the fragment ions. Phosphorylated peptides were measured and identified by LC–MS/MS. We extracted phosphorylated peptides that exceeded 10,000 in the peak area value of A1 (ERE-GFP-positive cell) and picked up those that were 5-fold over the A1/MCF-7-E10 cell value (Supplemental Table 1). Phosphoproteomic data were analyzed by KeyMolnet software, which is a new approach to mechanistic analysis and was developed by the Institute of Medicinal Molecular Design, Inc. (IMMD) [14]. Known molecular data and our phosphoproteomic data were combined with this software and shown as a molecular network. We performed a "start point to end point search" by selecting phosphorylated peptides identified by proteomics as starting points and estrogen receptor alpha as an end point.

Supplementary material related to this article can be found, in the online version, at http://dx.doi.org/10.1016/j.jsbmb.2013.08.012.

2.10. Statistical analyses

The Student's *t*-test was used to assess the significance of differences between two groups performed in triplicate. Data were expressed as means ± SD. $p < 0.05$ was considered significant.

3. Results

3.1. Establishment of estrogen-deprivation-resistant ERE-GFP-positive and negative MCF-7 cell lines

MCF7-E10 cells that had been stably transfected with the ERE-GFP reporter plasmid [8] were used as the parental cells to isolate estrogen-deprivation-resistant MCF-7 cells. They were cultured in DCC-treated FCS medium for at least 3 months. Among the surviving cells, ERE-GFP-expressing colonies and ERE-GFP-non-expressing colonies in the estrogen-deprivation (ED) medium were separately picked up (37 colonies) under a fluorescent microscope (Fig. 1A), and several cell lines (10 clones) were established by subsequent culture and passage in ED medium. The ERE-GFP activities of these established cell lines were analyzed according to the previously described method [8–10]. Fig. 1B shows representative examples of the activity of each of these EDR ERE-GFP-positive and ERE-GFP-negative MCF7-E10 cells. Three clones (A1, A2, C5) that had higher activity than the others and another three clones (A4, C7, K2) that showed almost no ERE-GFP activity were selected and used for the following experiments. ERE-GFP activity was strongly inhibited by the addition of the pure antiestrogen fulvestrant, which indicated the involvement of ERα in the activity of these ERE-GFP-expressing cells (Fig. 1B and C). In addition, the conventional ERE-luciferase assay of these EDR-MCF-7 cells also showed high ER activity in GFP-positive cells, but low activity in GFP-negative cells (Supplemental Data 1). The estrogen dependence of cell growth in these EDR-MCF7-E10 cells was then analyzed. Both ERE-GFP-positive and -negative EDR cells showed much lower sensitivity to estrogen than parental cells (Fig. 1D).

Supplementary material related to this article can be found, in the online version, at http://dx.doi.org/10.1016/j.jsbmb.2013.08.012.

3.2. Overexpression of ERα in GFP-positive EDR-MCF7-E10 cells

ERα protein expression in these cell lines revealed the significant induction of ERα expression in all three ERE-GFP-positive cell lines (Fig. 2A and B). Previous reports showed the induction of human epidermal growth factor receptor type 2 (Her2) and epidermal growth factor receptor (EGFR) expression in estrogen-deprivation-resistant cells [15,16]. However, none of our EDR-MCF-7-E10 cell lines showed the significant up-regulation of Her2 or EGFR expression (Fig. 2A).

3.3. Effect of antiestrogens on EDR cells

The effect of antiestrogens on the cell growth of these EDR cells was evaluated as shown in Fig. 2C. The growth of A1, A2, and C5 was inhibited by all antiestrogens, while that of A4, C7 and K2 was not inhibited by 4-OHT. A4 and K2 cell growth was inhibited by fulvestrant, which suggested that it had a stronger effect on the proliferation of these cells than that of tamoxifen. Interestingly, the growth of all ERE-GFP negative cells was significantly diminished by toremifene. These results indicate that ERE-GFP-positive EDR cells were responsive to antiestrogens for hormonal therapy. In contrast, the effect of these drugs was weaker in ERE-GFP-negative ones than in ERE-GFP-positive EDR cells.

3.4. Expression of endogenous ER-target genes in EDR cells

The expression of the endogenous ERα target genes, *pS2*, *PgR*, *EGR3* [17], *Bcl-2* and *CyclinD1* was analyzed by real-time RT-PCR in these cell lines. As shown in Fig. 3, ERE-GFP-positive cells

regularly because E10 was difficult to grow in estrogen-deprived medium. Cells were treated with the PI3K inhibitor, LY294002 (DMSO, 1 μM, 5 μM, 10 μM), for 4 days. The number of cells was counted using a Coulter Counter. All data shown as a percentage of the control are means ± SD of triplicate determinations of three independent experiments. (D) The ER activity of GFP-positive cells was inhibited by the PI3K inhibitor. Cells were cultured as mentioned above for (C), and treated with LY294002 (5 μM) for 4 days. The number of cells expressing GFP was counted under fluorescence microscopy. Data are shown as a percentage of GFP-positive cells among 100 counted cells. (E) ER.A/B-dependent transcriptional activities treated with LY294002 in MCF-7-E10 cells and GFP-positive EDR cells. MCF-7-E10 cells and EDR cells were seeded at a density of 5×10^4 cells per 6-cm dish in estrogen-deprived medium and cultured for 24 h. After the co-transfection of the pCMX-GAL4-N-ER.A/B, tk-GALpx3-Luc, or pRL-TK-Luc control plasmid in DCC-FCS medium for 1 h, cells were treated with LY294002 (5 μM) and cultured for 24 h. Cell lysates were assayed for luciferase activity. Statistical analysis of the indicated averages was performed using the Student's *t*-test where $p < 0.05$ (B and D), $p < 0.01$ (C).

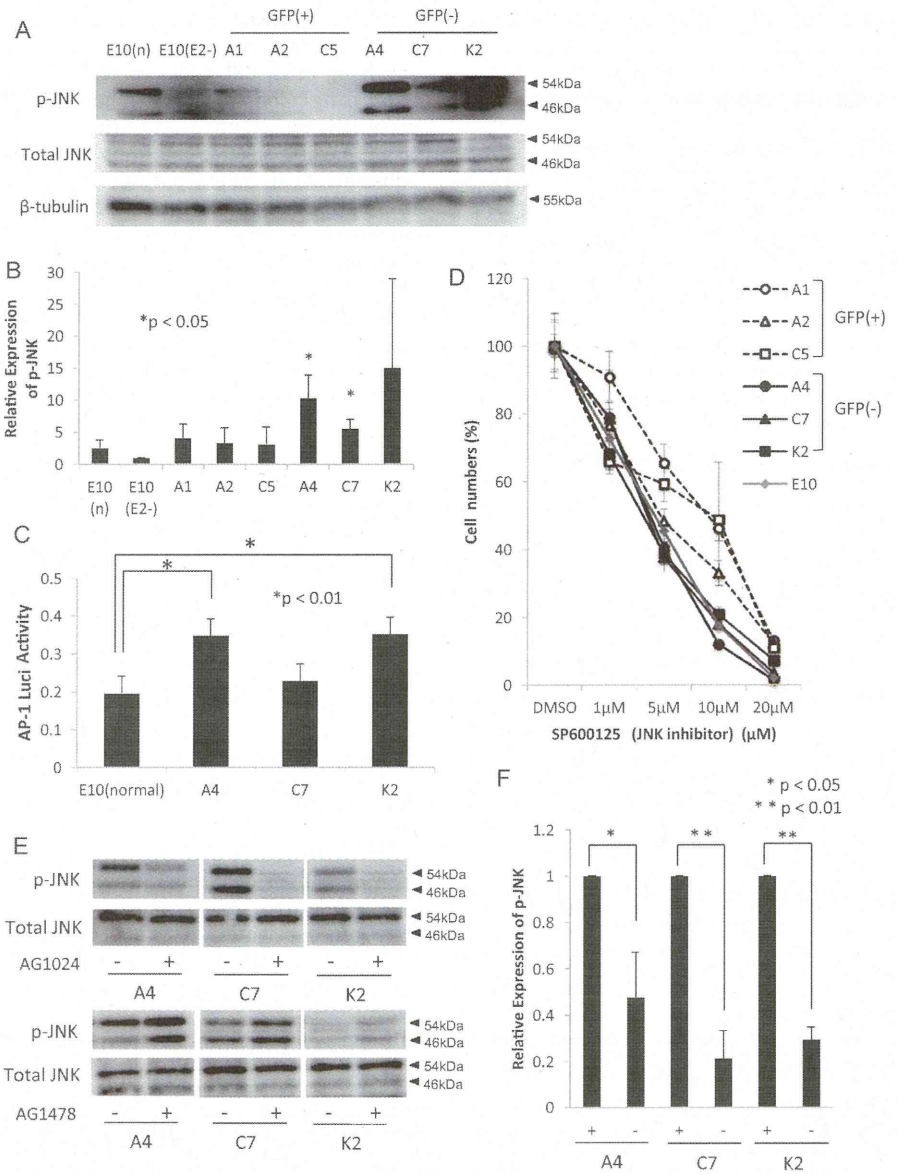

Fig. 5. The IGF1R-JNK pathway may contribute to the proliferation of GFP-negative EDR cells. (A) Western blot analysis using whole-cell lysates from MCF-7-E10 and EDR cells was performed using antibodies against JNK, p-JNK and β-tubulin as described in Section 2. (B) Densitometry results on p-JNK blots. Densitometry was performed on three blots and the results were indicated as values relative to the intensity with E10 (E2−). Statistical analysis of the indicated averages was performed using the Student's *t*-test, $p < 0.05$. (C) The AP-1 luciferase assay was carried out in MCF-7-E10 cells and GFP-negative EDR cells (A4, C7, K2) showing the phosphorylation of high levels of JNK as described in Section 2. Statistical analysis of the indicated averages was performed using the Student's *t*-test, $p < 0.01$. (D) The growth of GFP-negative cells was inhibited by the JNK inhibitor. MCF-7-E10 cells were plated at 5.0×10^3 cells/well into a 24-well plate and were cultured in RPMI1640 with 10% FCS. EDR cells (A1, A2, C5, A4, C7, K2) were also plated at 5.0×10^3 cells/well into a 24-well plate and were cultured in phenol red-free RPMI1640 with 10% DCC-FCS. Cells were treated with the JNK inhibitor, SP600125 (DMSO, 1 μM, 5 μM, 10 μM, 20 μM) for 5 days. The number of cells was counted using a Coulter Counter. (E) Phosphorylated JNK were suppressed by the IGF-1R inhibitor. GFP-negative EDR cells (A4, C7, K2) were plated at 1.0×10^5 cells/6-cm dish and were cultured in phenol red-free RPMI1640 with 10% DCC-FCS. After 3 days, the cells were incubated with DMSO as a control and with 10 μM AG1024 and AG1478 for 1 h. Western blot analysis using these whole-cell lysates from GFP-negative EDR cells were performed using the antibody against p-JNK. (F) Densitometry results on p-JNK blots inhibited by the IGF-1R inhibitor, AG1024. Densitometry was performed on the three blots and the results were indicated as values relative to the intensity with the control. Statistical analysis of the indicated averages was performed using the Student's *t*-test, $p < 0.01$.

such as A1, A2, and C5 strongly expressed *pS2*, *PgR*, *EGR3* [17] and *Bcl-2*, while the ERE-GFP-negative cells, A4, C7 and K2, did not show any significant mRNA expression of these ER-target genes. Since ER-expressing breast cancer was previously suggested to be less sensitive to chemotherapy [18], the strong expression of *Bcl-2* observed in ERE-GFP-positive EDR cells may be a useful biomarker for the treatment of recurrent breast cancer following hormonal therapy. Furthermore, the expression of *CyclinD1* in all ERE-GFP-positive and -negative cells was equivalent to that of the parental cells. These results indicate that ER transcription in ERE-GFP-expressing cells was constitutively activated in an estrogen-independent manner, while ERE-GFP-negative cells mostly lost ER transcriptional activity.

Taking these findings together with other results, ERE-GFP-positive EDR cells were shown to be dependent on the constitutive activation of ERα in terms of their growth, while the proliferation of ERE-GFP-negative cells could be supported by another signaling pathway.

3.5. Phosphorylation of ERα on Ser167 by the PI3K-Akt pathway may contribute to estrogen-independent proliferation in the ERE-GFP-positive EDR cells

ERα was previously shown to be activated by protein phosphorylation [19–22]. We analyzed intracellular signaling factors, such as Erk and Akt, which had been reported to be related to estrogen signaling, and investigated the phosphorylation status of ERα in ERE-GFP-positive and -negative EDR cells. The status of Akt on Thr308 appeared to be increased in A1, A2, and C5 cells, while the expression of total Akt did not change (Fig. 4A and B). However, we could not find a marked change in the total and phosphorylation status of p44/42 MAPK (Erk1/2) in these cells (Fig. 4A). On the other hand, among the ERE-GFP-negative cells, K2 cells had a high p44/42 MAPK (Erk1/2) phosphorylation status (Supplemental Data 2A). ERE-GFP-positive cells showed higher phosphorylation levels of ERα on Ser167, but not on Ser118 (Fig. 4A and B). These results suggested that activation of the PI3K-Akt signal phosphorylated ERα on Ser167 in breast cancer cells. Furthermore, growth was significantly inhibited by LY294002, a PI3K inhibitor, in ERE-GFP-positive cells (Fig. 4C), which indicated that the PI3K-Akt pathway may be involved in their growth and ER constitutive activation. On the other hand, the proliferation of ERE-GFP-negative cells was not significantly diminished by LY294002 (Supplemental Data 2B). We then examined whether PI3K-Akt pathway signaling activated ERα in ERE-GFP-positive EDR cells using an ERE-GFP assay. Fig. 4D shows that the activity of ERα in these cells was inhibited by LY294002. These results suggest that the phosphorylation of ERα on Ser167 by the PI3K-Akt pathway may contribute to the estrogen-independent and constitutive activation of ERα in ERE-GFP-positive EDR cells.

Supplementary material related to this article can be found, in the online version, at http://dx.doi.org/10.1016/j.jsbmb.2013.08.012.

ERα has two transactivation domains, A/B and E, which mediate ligand-independent and ligand-dependent transactivation, respectively. Phosphorylation site Ser167 of ERα is included in the A/B domain. We investigated whether ERE-GFP-positive cells showed constitutive activation of the A/B domain by PI3K-Akt pathway relative to the parental cells. To analyze transcriptional activities of the A/B and E domains in ERE-GFP-positive cells, we performed a luciferase assay using expression vectors containing either an A/B domain or E domain fused to a GAL4-DNA-binding domain, together with the reporter plasmid with the GAL4-DBD response element [11]. As expected, activation of the E domain was induced by E_2 in MCF-E10 cells, while that of the A/B domain was not (data not shown). Under estrogen-deprivation conditions, the A/B domain-dependent activity of ERE-GFP-positive cells was higher than that of parental cells (Fig. 4E). In addition, A/B domain-dependent activity was inhibited by LY29402 in ERE-GFP-positive EDR cells (Fig. 4E). These results suggested that the PI3K-Akt pathway activated the ligand-independent transactivation domain of ERα in ERE-GFP-positive EDR cells.

3.6. Constitutive JNK activation of GFP-negative EDR cells

We further analyzed the representative proteins involved in the intracellular phosphorylation signaling pathway that had been reported to be related to estrogen signaling, and found that only c-Jun N-terminal kinase (JNK) was constitutively activated in ERE-GFP-negative EDR cells (Fig. 5A and B). Activator protein 1 (AP-1) luciferase activity of A4 and K2 cells was significantly higher than that of E10 cells (Fig. 5C). Furthermore, as shown in Fig. 5D, the JNK inhibitor, SP600125, more effectively inhibited the growth of ERE-GFP-negative cells than that of ERE-GFP-positive cells. These results suggest that the JNK-related signaling pathway could be important for the survival of ERE-GFP-negative and ER-independent MCF-7 cells.

3.7. The IGF1R-JNK pathway may be important for the proliferation of ERE-GFP-negative cells

To explore the upstream signals of the JNK pathway in these cells, we examined whether EGFR and insulin-like growth factor receptor (IGF1R) were involved in the phosphorylation of JNK in ERE-GFP-negative EDR cells. Fig. 5E shows that p-JNK were significantly down-regulated after treatment with the IGF1R inhibitor, AG1024, in these three EDR cells (Fig. 5E and F). On the other hand, the expression of p-JNK was not altered or slightly increased by treatment with the EGFR inhibitor, AG1478. Considering that JNK may be an important factor for the growth of ERE-GFP-negative EDR cells (Fig. 5D), these results suggest that the IGF-1R-JNK signal pathway may be a significant mechanism for the proliferation of these cells; however, further studies will be needed to elucidate these details.

4. Discussion

The majority of women suffering from breast cancer have ER-positive tumors. Thus, hormonal therapy targeting ERα or its signaling pathway could be an efficacious therapeutic strategy for breast cancer. However, approximately one-third of ER-positive patients do not respond to hormonal therapy in an adjuvant setting. They show resistance to antiestrogens or aromatase inhibitors. In the last three decades, tamoxifen has been used as a standard antiestrogen drug in hormonal therapy for breast cancer [23]. Thus, numerous studies on tamoxifen resistance have been conducted and several mechanisms have been postulated [24,25]. However, to date, none of these has practically contributed to a clinical benefit for breast cancer patients. In recent years, the superior efficacy of third generation aromatase inhibitors has been indicated in several randomized clinical trials [3]. Thus, this type of drug is now widely used globally for the treatment of ER-positive breast cancer. The strategy of this type of drug is the blockade of estrogen production in cancerous regions to inhibit the action of estrogen in cancer cells. However, AI-resistant patients have often been reported, even in ER-positive cases. The acquisition of resistance to estrogen deprivation could be a major mechanism in these cases. Accordingly, studies on estrogen-deprivation resistance have also been performed by several laboratories; however, no consensus regarding the mechanisms involved has been obtained. The reason for this may be that multiple mechanisms may have all played a role in previous studies using estrogen-deprivation-resistant cells. In this study, we used EDR cells, which were transfected with the ERE-GFP reporter gene, and demonstrated for the first time that more than two clearly distinct mechanisms exist in estrogen-deprivation resistance. Furthermore, these results suggest that two mechanisms may simultaneously occur, which means that breast cancers with different AI-resistance mechanisms can concomitantly occur and mingle in an individual breast cancer case. This phenomenon may be involved in the acquisition of further resistance for a second or third therapy. Therefore, it is important to elucidate the detailed mechanisms for developing an appropriate therapy.

We subsequently characterized our EDR cells, which appeared to have distinct mechanisms of resistance. ERE-GFP-positive EDR cells showed the overexpression of ERα and maintained high ER activity in estrogen-deprivation conditions. The up-regulation of ER-target genes confirmed that these cells showed ER-dependent proliferation. Furthermore, significant induction of the MAP kinase pathway was not observed in our ERE-GFP-positive EDR cell lines. On the other hand, Campbell et al. reported that activation of

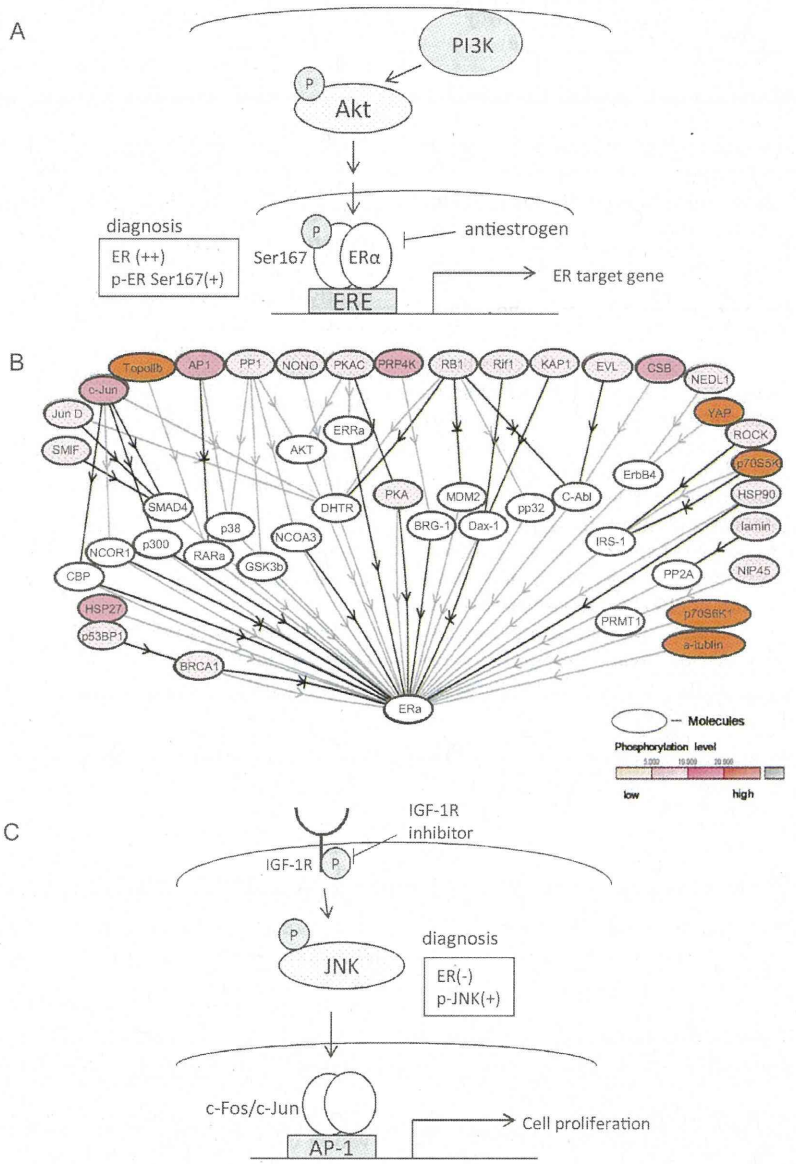

Fig. 6. Models of the mechanisms for estrogen-independent growth in GFP-positive and -negative EDR cells. (A) In GFP-positive EDR cells, the overexpression of ERα and activation of Akt phosphorylated ERα on Ser167, inducing constitutive ERα activation and ERα-mediated transcription. (B) The possible signal pathway connected to ERα involving molecules that were phosphorylated more in GFP-positive cells (A1) than in parental MCF-7-E10 cells were investigated by KeyMolnet analysis in Section 2. These pathways indicated several possibilities for the mechanisms of ER activity in ERE-GFP-positive EDR cells. The red circle shows molecules with higher phosphorylation levels in A1 than in MCF-7-E10; the lines show that the relationship was confirmed by a review (black lines) or a single study (gray lines). (C) In GFP-negative EDR cells, the IGF-1R pathway induced the activation of JNK and significant activation of AP-1 transcription activity. This signal pathway may be important for the survival of ER-independent MCF-7 cells.

the PI3K-Akt signal that phosphorylates ERα on Ser167 in breast cancer cells is implicated in tamoxifen resistance [20]. However, ERE-GFP-positive EDR cells that showed a marked change in the phosphorylation status of ERα on Ser167 and Akt on Thr308 were responsive to antiestrogen drugs, such as tamoxifen. A possible reason for some discrepancies between our results and previous studies is that the estrogen-deprivation-resistant cells in previous studies may have exhibited multiple mechanisms. The new strategy, using ERE-GFP-introduced EDR cells, established by cloning from a single colony, enabled us to avoid this complication. Another report in which the phosphorylation of ERα on Ser167 induced binding on ERE and transcriptional activation [26] also explains the high ER activity in our ERE-GFP-positive EDR cells. Additionally, the results of immunostaining using specimens from breast cancer patients showed that patients with the phosphorylation of high levels of ERα on Ser167 were responsive to antiestrogen drugs for hormonal therapy [27], which is consistent with the effect of antiestrogens on the cell growth of ERE-GFP-positive EDR cells. The reduction in ER activity and growth in ERE-GFP-positive EDR cells by inhibiting the PI3K-Akt signal pathway also suggests that the phosphorylation of ERα on Ser167 by the PI3K-Akt pathway may contribute to the constitutive activation of ERα and proliferation in ERE-GFP-positive EDR cells (Fig. 6A). Taken together, these results suggest that the overexpression and phosphorylation of ERα on Ser167 may be a useful diagnostic marker for cases that are ER-dependent.

We also carried out comprehensive phosphoproteomic analysis [12,13] as described in Section 2 to explore the mechanism

of estrogen-independent and constitutive activation of ERα in ERE-GFP-positive EDR cell lines by another approach. Comprehensive phosphoproteomic and pathway analyses of these cells supported our hypothesis that the PI3K-Akt pathway phosphorylates ERα (Fig. 6B) and suggested that other signaling pathways may be involved in the activation of ERα. Previous studies have indicated that the PKA signal pathway was important for tamoxifen resistance in breast cancer cells [28–30]. Methods such as comprehensive phosphoproteomic analysis may contribute to identifying the particular molecules related to these mechanisms in detail for the next step.

From a clinical perspective, these mechanisms of estrogen-deprivation resistance in ERE-GFP-positive EDR cells suggest that SERM and SERD may be more effective for AI-resistant breast cancer showing ERα overexpression and the phosphorylation of ERα on Ser167.

On the other hand, the three ERE-GFP-negative cell lines could have acquired estrogen-independent and ER-independent growth mechanisms. The expression of ER-target genes was downregulated and antiestrogens were often less effective in ERE-GFP-negative EDR cells than in ERE-GFP-positive cells. Tamoxifen inhibits the binding of estrogen to ER, while fulvestrant has a similar effect to tamoxifen and also degrades the ER receptor. In Fig. 2B, A4 and K2 were significantly inhibited by fulvestrant, which suggests that it is more effective in these cells than tamoxifen considering the mechanisms of this drug. Interestingly, the growth of all ERE-GFP negative cells was diminished by toremifene, which had the same effect as tamoxifen. Two reasons have been suggested for this phenomenon. Firstly, the concentration of toremifene used in this experiment was high, and was previously shown to be effective in some postmenopausal breast cancer patients [31]. Secondly, several reports have suggested that toremifene inhibited the growth of hormone-dependent MCF-7 tumors and anaplastic thyroid carcinoma cell lines via IGFR [32,33]. In addition, IGF1R was suggested to be related to the growth of ERE-GFP-negative cells in Fig. 5. Considering these results together with previous reports, the inhibition of growth in ERE-GFP-negative cells by toremifene could be via IGF1R.

These cell lines showed the robust induction of phosphorylated JNK and significant activation of AP-1 transcription activity. Since the JNK pathway has been shown to play a crucial role in the growth and development of breast cancer [34], the estrogen-deprivation resistance and ER signal-independence of these cells may have been acquired by the constitutive activation of this signaling pathway. Primary breast cancer is known to overexpress IGF1R, which is phosphorylated in many breast cancer subtypes [35]. A previous study has shown that IGF1R signaling is involved in the antiestrogen resistance of breast cancer cells [36]. In this study, we showed that the inhibition of IGF1R activity by AG1024 decreased phosphorylated JNK (Fig. 5E and F) and the proliferation of these cells was inhibited by SP600125 (Fig. 5D), which suggested that the IGF1R-JNK signal pathway induced the proliferation and survival of ERE-GFP-negative cells (Fig. 6C). On the other hand, K2 caused a marked change in the phosphorylation status of p44/42 MAPK (Erk1/2) (Supplemental Data 2A), and this result indicated that MAPK signal pathways may be partly involved in the activation of these cells. The involvement of the IGF-1R-JNK-AP-1 pathway in ERE-GFP-negative cells, as indicated by an in vitro experiment, suggests the possibility of a new molecular target to overcome hormonal therapy resistance. The activation of JNK may be a diagnostic marker and therapeutic target for the recurrence of luminal-type breast cancer. Considering these results together with previous reports, the molecular mechanism for the acquisition of estrogen-deprivation resistance is not uniform, and various intercellular signaling pathways could impact on the survival, growth, and development of hormonal therapy-resistant breast cancer. The distinction of these mechanisms of estrogen-deprivation resistance may contribute to the individualization of breast cancer to determine eligibility criteria for recurrent patients and the provision of appropriate therapy.

Conflict of interest

The authors declare no conflict of interest.

Acknowledgments

This study was supported in part by a Grant-in-Aid for Scientific Research from the Ministry of Education, Science, Sports and Culture, Japan; a Grant-in-Aid for Cancer Research from the Ministry of Health, Labor and Welfare, Japan; the Program for Promotion of Fundamental Studies in Health Science of the National Institute of Biomedical Innovation (NIBIO); and a grant from the Smoking Research Foundation.

References

[1] K. Strasser-Weippl, P.E. Goss, Advances in adjuvant hormonal therapy for postmenopausal women, J. Clin. Oncol. 23 (8) (2005) 1751–1759.
[2] R.B. Riggins, R.S. Schrecengost, M.S. Guerrero, A.H. Bouton, Pathways to tamoxifen resistance, Cancer Lett. 256 (1) (2007) 1–24.
[3] M. Baum, A. Buzdar, J. Cuzick, J. Forbes, J. Houghton, A. Howell, T. Sahmoud, ATAC (Arimidex, Tamoxifen Alone or in Combination), Trialists' Group, Anastrozole alone or in combination with tamoxifen versus tamoxifen alone for adjuvant treatment of postmenopausal women with early-stage breast cancer: results of the ATAC (Arimidex, Tamoxifen Alone or in Combination) trial efficacy and safety update analyses, Cancer 98 (9) (2003) 1802–1810.
[4] W. Yue, J.P. Wang, M.R. Conaway, Y. Li, R.J. Santen, Adaptive hypersensitivity following long-term estrogen deprivation: involvement of multiple signal pathways, J. Steroid Biochem. Mol. Biol. 86 (3–5) (2003) 265–274.
[5] G.J. Sabnis, D. Jelovac, B. Long, A. Brodie, The role of growth factor receptor pathways in human breast cancer cells adapted to long-term estrogen deprivation, Cancer Res. 65 (9) (2005) 3903–3910.
[6] L.A. Martin, I. Farmer, S.R. Johnston, S. Ali, M. Dowsett, Elevated ERK1/ERK2/estrogen receptor cross-talk enhances estrogen-mediated signaling during long-term estrogen deprivation, Endocr. Relat. Cancer 12 (Suppl. 1) (2005) S75–S84.
[7] R.J. Santen, R.X. Song, S. Masamura, W. Yue, P. Fan, T. Sogon, S. Hayashi, K. Nakachi, H. Eguchi, Adaptation to estradiol deprivation causes up-regulation of growth factor pathways and hypersensitivity to estradiol in breast cancer cells, Adv. Exp. Med. Biol. 630 (2008) 19–34.
[8] Y. Yamaguchi, H. Takei, K. Suemasu, Y. Kobayashi, M. Kurosumi, N. Harada, S. Hayashi, Tumor-stromal interaction through the estrogen-signaling pathway in human breast cancer, Cancer Res. 65 (11) (2005) 4653–4662.
[9] M. Matsumoto, Y. Yamaguchi, Y. Seino, A. Hatakeyama, H. Takei, H. Niikura, K. Ito, T. Suzuki, H. Sasano, N. Yaegashi, S. Hayashi, Estrogen signaling ability in human endometrial cancer through the cancer-stromal interaction, Endocr. Relat. Cancer 15 (2) (2008) 451–463.
[10] T. Gohno, Y. Seino, T. Hanamura, T. Niwa, M. Matsumoto, N. Yaegashi, H. Oba, M. Kurosumi, H. Takei, Y. Yamaguchi, S. Hayashi, Individual transcriptional activity of estrogen receptors in primary breast cancer and its clinical significance, Cancer Med. 1 (3) (2012) 328–337.
[11] T. Sakamoto, H. Eguchi, Y. Omoto, T. Ayabe, H. Mori, S. Hayashi, Estrogen receptor-mediated effects of tamoxifen on human endometrial cancer cells, Mol. Cell. Endocrinol. 192 (1/2) (2002) 93–104.
[12] K. Imami, N. Sugiyama, M. Tomita, Y. Ishihama, Quantitative proteome and phosphoproteome analyses of cultured cells based on SILAC labeling without requirement of serum dialysis, Mol. Biosyst. 6 (3) (2010) 594–602.
[13] N. Sugiyama, T. Masuda, K. Shinoda, A. Nakamura, M. Tomita, Y. Ishihama, Phosphopeptide enrichment by aliphatic hydroxy acid-modified metal oxide chromatography for nano-LC–MS/MS in proteomics applications, Mol. Cell. Proteomics 6 (6) (2007) 1103–1109.
[14] H. Sato, S. Ishida, K. Toda, R. Matsuda, Y. Hayashi, M. Shigetaka, M. Fukuda, Y. Wakamatsu, À. Itai, New approaches to mechanism analysis for drug discovery using DNA microarray data combined with KeyMolnet, Curr. Drug Discov. Technol. 2 (2) (2005) 89–98.
[15] L.A. Martin, I. Farmer, S.R. Johnston, S. Ali, C. Marshall, M. Dowsett, Enhanced estrogen receptor (ER) alpha, ERBB2, and MAPK signal transduction pathways operate during the adaptation of MCF-7 cells to long term estrogen deprivation, J. Biol. Chem. 278 (33) (2003) 30458–30468.
[16] R.I. Nicholson, J.M. Gee, J. Knowlden, R. McClelland, T.A. Madden, D. Barrow, I. Hutcheson, The biology of antihormone failure in breast cancer, Breast Cancer Res. Treat. 80 (Suppl. 1) (2003) S29–S34, discussion S35.
[17] A. Inoue, Y. Omoto, Y. Yamaguchi, R. Kiyama, S.I. Hayashi, Transcription factor EGR3 is involved in the estrogen-signaling pathway in breast cancer cells, J. Mol. Endocrinol. 32 (3) (2004) 649–661.